## TITLE

**Parameter optimization for laser patterning of CVD diamond: characterization of surface morphology**

## AUTHORS

John Smedley[a)], Triveni Rao and Qiong Wu
*Brookhaven National Laboratory, Upton, NY 11973*

Jen Bohon
*Case Western Reserve University, Cleveland, OH 44106*

## ABSTRACT

As the use of diamond as a material for electronic and research applications increases, methods of patterning diamond will be required. In this work, single- and poly-crystalline synthetic diamond samples were exposed to laser beams of different energies, wavelengths and pulse durations. The effects of this exposure were characterized using optical microscopy, scanning electron microscopy and atomic force microscopy. The threshold ablation energy density for 266nm radiation with ~30ps pulse duration was measured to be ~14J/cm$^2$. The threshold for ~10ns pulses at the same wavelength was similar but the ablated area displayed larger surface damage. The surface damage and the threshold energy increases significantly for 532 and 1064nm radiation. Ablation performed using 213nm radiation produced the most uniform surface. Changes in the ablated surface are presented in detail.

## I. INTRODUCTION

Due to the unique combination of mechanical, optical, electronic and thermal properties, diamond is an ideal material for a wide variety of purposes. Recent advances in the chemical vapor deposition (CVD) process have increased the availability of high-purity diamond for optical and electronic applications. For some of these applications, such as lenses[1] and diamond electron sources,[2] the diamond needs to be patterned with micron or sub-micron sized features. Other methods of milling and pattering diamond exist,[3-5] but tend to be slower than laser ablation, which is important if significant thickness reduction or large aspect ratios are required. Previous studies of laser ablation of diamond[6-10] were typically conducted with excimer lasers having ns pulse durations. We have investigated laser ablation of both single- and poly-crystalline CVD diamond using laser pulses of ps and ns duration and wavelengths of 213, 266, 532 and 1064nm. The ablated samples were characterized using a number of techniques, including optical microscopy, SEM, AFM, Raman spectroscopy, FTIR, NEXAFS and x-ray diffraction. This manuscript is the first part of a series detailing this characterization. In the subsequent sections, the etching process and the results observed with the optical microscope, SEM and AFM are presented. Investigation of the non-diamond carbon residue formed on the diamond surface during the laser ablation process with NEXAFS and FTIR is presented in a second manuscript.[11] Studies of the stress induced in diamond due to laser ablation and techniques to minimize/eliminate the stress are ongoing.

## II. EXPERIMENTAL DETAILS

Two lasers with pulse durations of 30ps and 10ns, both operating at a fundamental wavelength of 1064nm and a frequency of 10Hz, were used for the ablation. The ps laser is an actively and passively mode-locked Nd:YAG oscillator followed by a pulse selector and double pass amplifier, (Leopard series,

Continuum Lasers) capable of delivering 125mJ at 10Hz in a pulse duration of 60ps at 1064nm. The fourth harmonic (266nm) is obtained by two successive doubling crystals which provide up to 13mJ energy in 30ps. The fifth harmonic (213nm) is generated via a 4+1 frequency mixing crystal. The energy on the target can be varied by either changing the pump power of the amplifier and/or using attenuating filters. The ns laser is a Q switched Nd:YAG (Quanta ray) capable of delivering up to 400mJ in 20ns pulse duration at a 10Hz repetition rate. Two doubling crystals were used in series to generate up to 200mJ of 532nm and 40mJ of 266nm radiation with pulse durations of 14 and 10ns respectively. The energy of the laser beam on the sample is adjusted by introducing appropriate filters into the beam path. The beam from either of these lasers is focused using a nominal 15cm lens to result in a 27±3μm focal spot size on the target (FWHM of Gaussian profile). The position of the sample at the focus was identified by the size of the laser beam back-reflected from the sample, and the spot size was measured by scanning an edge across the beam waist and measuring the transmitted power.

Five different polished CVD diamonds (Element Six) were used in the experiments. The two detector grade single-crystal diamonds (designated S1 and S2) had dimensions of 4x4x0.3mm and crystalline orientations 1,0,0 to the surface normal. Three electronic grade polycrystalline (designated P1, P2 and P3) diamonds were used; P1 and P2 were 10x10x0.3mm and P3 was 5x5x0.3mm. The diamonds were characterized before and after ablation via optical microscopy, scanning electron microscopy (SEM) and atomic force microscopy (AFM). The majority of SEM (JOEL 6500) images were obtained at a magnification of 100X with the samples set at a tilt to allow observation of the vertical features. The AFM measurements were made using an Easyscan 2 AFM (Nanosurf) to scan over 66x66μm areas at an image definition of 256 points per line at a speed of 1 second per line. The scans were performed with a 225x40x7μm silicon ACLA-50 cantilever (AppNano) with a tip radius of <10nm and a tip height of 12-16μm at a frequency of 145-230kHz and a spring constant of 20-95N/m. The open-source software Gwyddion was used to process the data. Fourier transform infrared spectroscopy (FTIR) confirmed the lack of detectable impurities in the unablated diamonds (data not shown).

The Klinger motion stage used to create the patterns in the diamonds rasters horizontally, then vertically in a 1x1 $mm^2$ square pattern with a specified step at a 1μm resolution. The ablation is performed in a vacuum system mounted on this stage. Typical vacuum pressure is better than 0.1mTorr, however some ablation was done with a partial pressure of oxygen introduced via a leak valve.

## III. RESULTS AND DISCUSSION

### A. Polycrystalline Diamond

*Wavelengths below the band gap*

In order to determine the threshold energy for ablation, P1 was raster scanned through a spot of area 200x200μm with a spacing of 10μm. The ps YAG was used at 266nm to create 17 such spots at increasing pulse energies (Fig. 1); the first observable surface change occurred at 84μJ (~14J/$cm^2$). Based on the results of this study, laser energies of ≥84μJ were chosen for subsequent ablations.

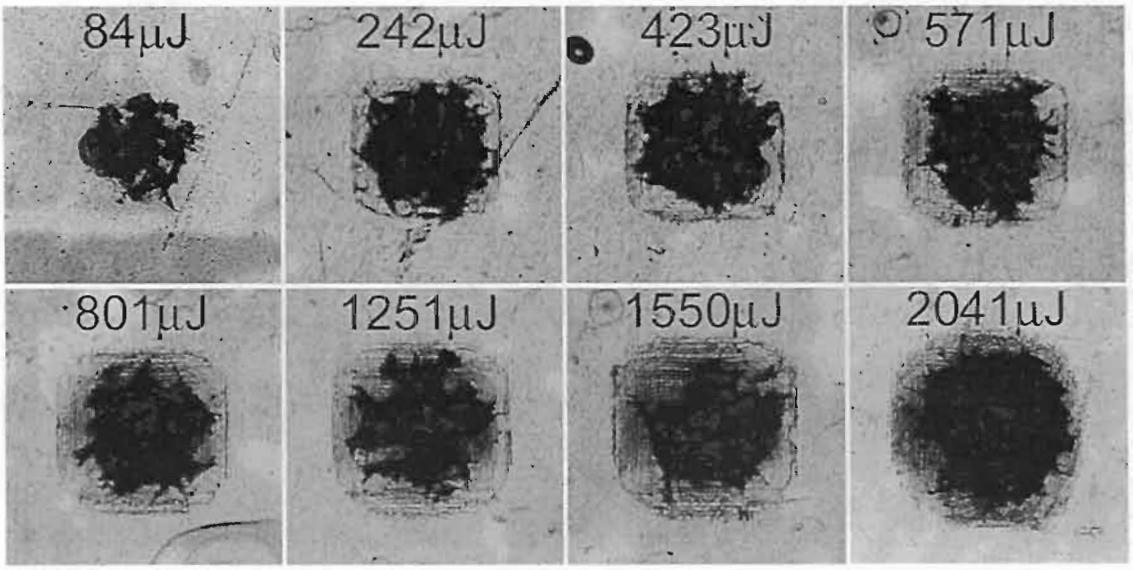


Figure 1. Damage threshold test. Optical microscope images of P1 ablated with increasing energy as labeled at 266nm with a 30ps pulse duration.

Keeping the same beam parameters, a 1x1mm$^2$ pattern of 50μm spacing was ablated into P1 (Fig. 2a) over a period of 70 minutes, with 11 passes over the same area. P3 was ablated using 90μJ of energy to create a 5μm step size raster pattern; 3 passes over the area took 193 minutes to complete (Fig. 2b).

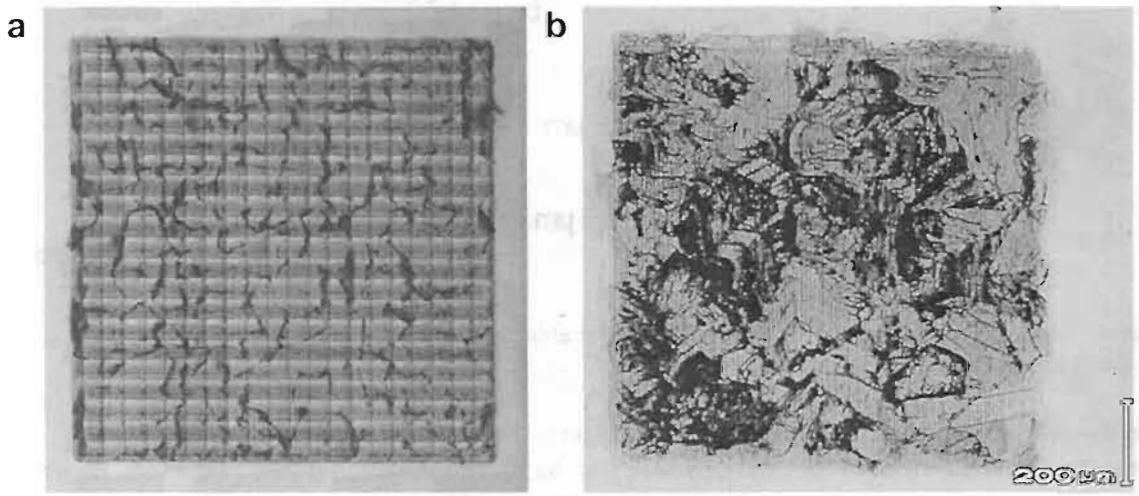


Figure 2. Optical microscope images of ~30ps 266nm laser ablation of (a) P1, 50μm raster spacing and (b) P3, 5μm raster spacing.

The patterns are visible in the optical images for both diamonds, but there are also signs of significant cracking and darkening of the surface. Raman spectra (data not shown) obtained from the darkened spots in the damage threshold test showed occasional weak structure at 1580cm$^{-1}$, corresponding to graphite, however this feature was not correlated to the laser energy used for ablation and was not present in all spots. Subsequent NEXAFS analysis[11] showed that the majority of the carbon was amorphous in nature. In order to remove this non-diamond layer, the diamond was subjected to ozone

cleaning (Fig. 3a). The SEM image of P1 (Fig. 3b) clearly reveals the 50μm spacing of the square pattern as well as very thin surface cracks upon close inspection.

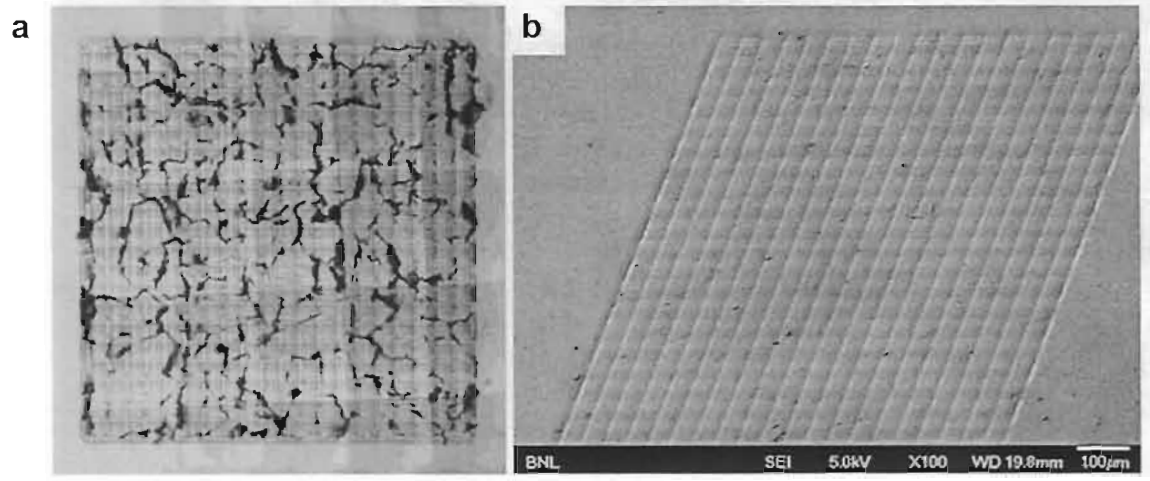


Figure 3. Optical (a) and SEM (b) images of P1 after ozone cleaning (see figure 2 for image before cleaning).

AFM measurements were performed on both the 50μm and 5μm scan regions to characterize the depth of the ablation. The 50μm pattern exhibited a relatively Gaussian profile reminiscent of the laser beam profile which varied from unablated to approximately 1μm in depth (Fig. 4).

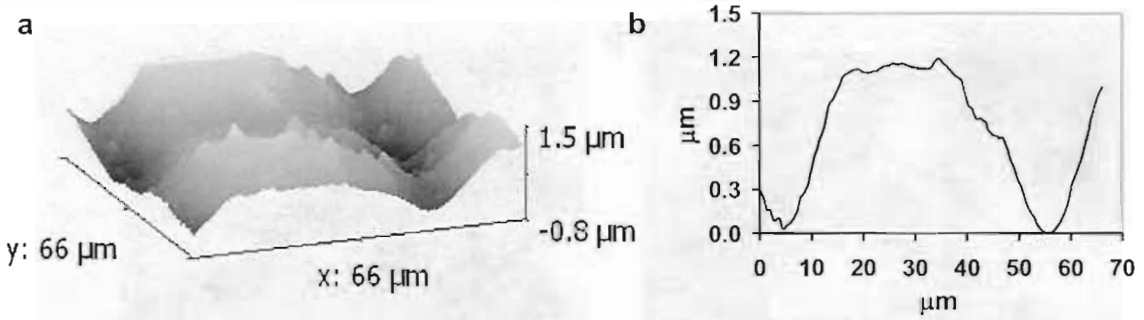


Figure 4. Atomic force microscopy of 50μm spacing laser ablation pattern on P1. Topographical image of scan (left); line scan indicating depth of groove (right).

Due to the overlapping ablation lines in the 5μm pattern, the variation in the profile is an order of magnitude smaller than that of the 50μm pattern (Fig. 5a,b). This variation is 25% of the total depth of ablation in this pattern as indicated by the edge step (Fig. 5c,d 5b). Several ablation attempts were performed in the presence of increasing levels of oxygen in the hopes that this would produce an initially cleaner surface. The vacuum chamber was backfilled with oxygen at base pressures of 14.2, 0.9, 0.1 and <0.0001 Torr using a leak valve and P1 was ablated at each of these pressures with a 50μm step. The introduction of oxygen did not yield any benefit.

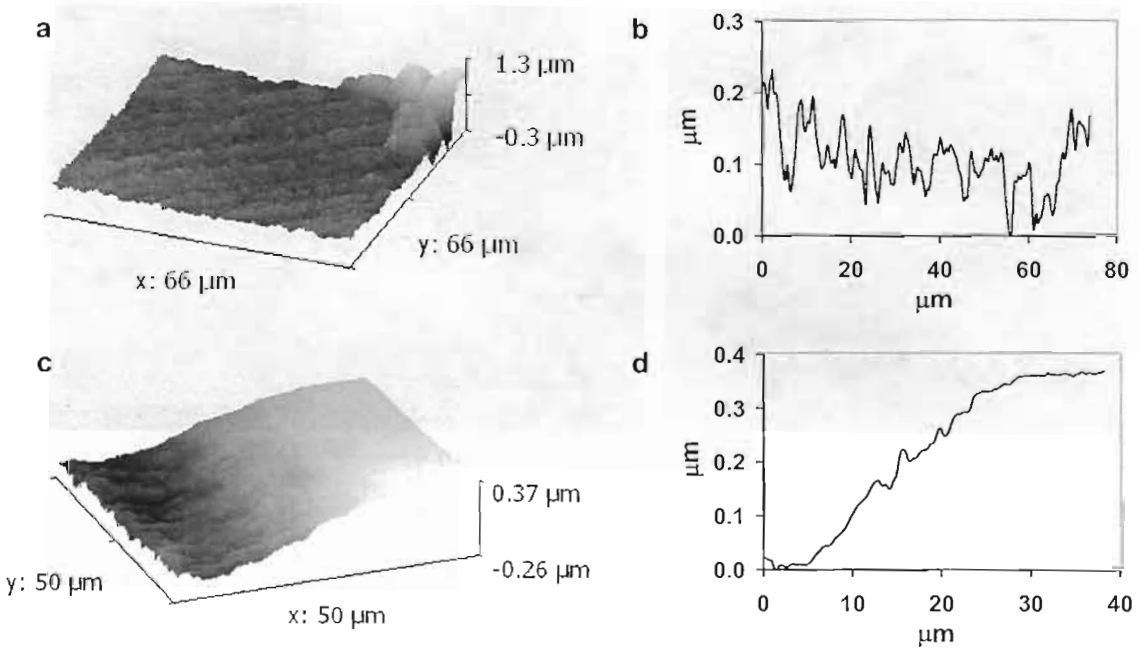


Figure 5. AFM images and line scans of 5µm spacing ~30ps 266nm laser ablation pattern on P3 (a and b) in the center of the pattern and (c and d) at the edge of the pattern.

Use of ns duration pulses required similar ablation energy (84µJ) to the ps duration radiation, but produced significant surface damage on P2 (Fig. 6). Both optical (Fig. 6a) and SEM (Fig. 6b) images clearly reveal the 50µm patterning step as well as craters on the order of 100µm wide non-uniformly spaced throughout the ablation area. The ablation depth profile for this radiation in areas not interrupted by craters is ~3µm, as indicated by the AFM scan (Fig. 6c,d).

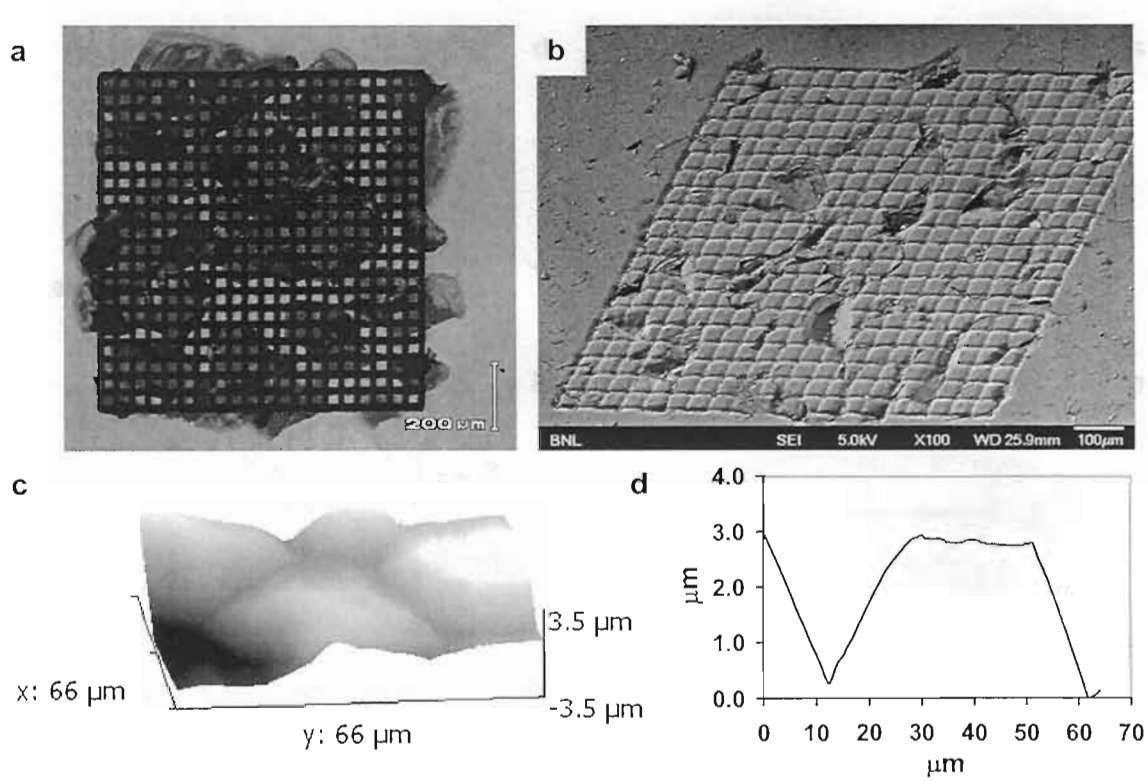


Figure 6. (a) Optical image (b) SEM image (c) AFM image and (d) AFM line scan of ~20ns 266nm ablation of P2.

Six 1x1mm$^2$ areas were ablated with background oxygen levels from vacuum to 1atm (Fig. 7). As was the case for ps duration radiation, the presence of oxygen during the ns duration ablation was not found to have a significant impact and thus use of this process was discontinued.

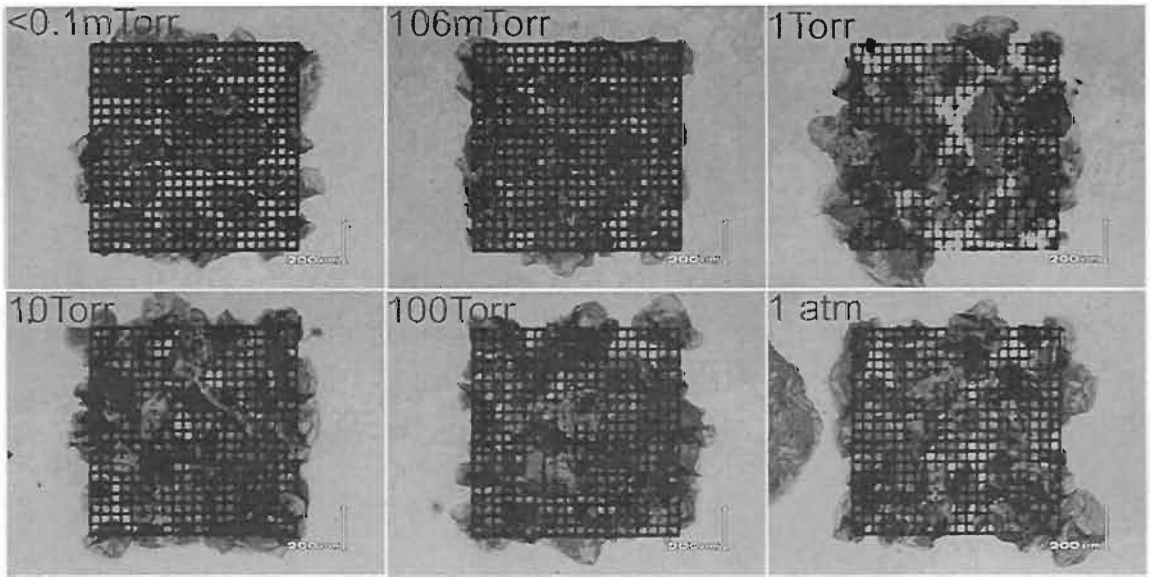


Figure 7. Optical microscope images of P2 ablated with ~10ns 266nm radiation in the presence of increasing oxygen partial pressures as labeled.

Use of 532nm radiation required an increase in the ablation energy to 132μJ in order to surpass the diamond damage threshold. Although the raster pattern is observable in some areas (Fig. 8), ablation with this setting is quite destructive, non-uniformly removing large regions of the diamond surface. With infrared radiation (1064nm), the damage threshold was never reached under the conditions used (up to 214μJ).

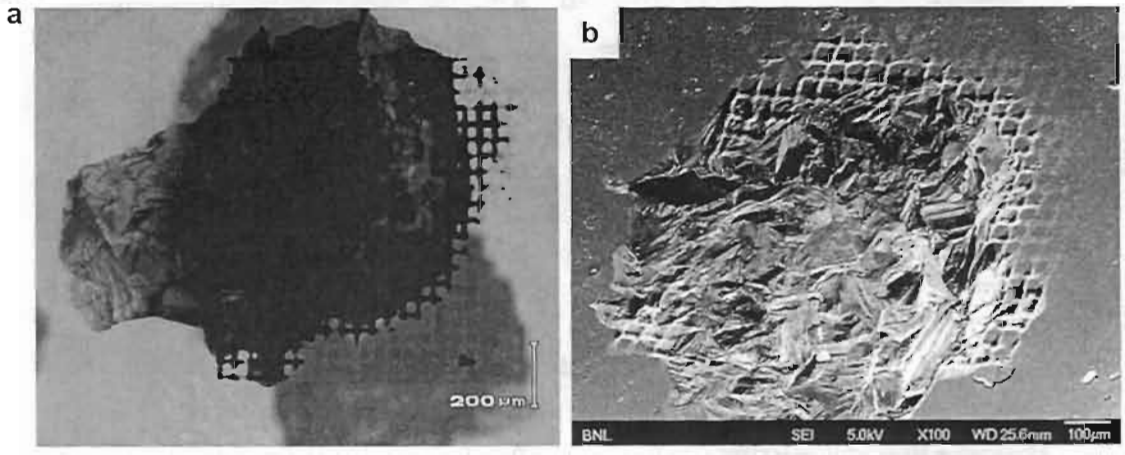


Figure 8. (a) Optical image and (b) SEM image of 532nm ablation of P2.

*Wavelengths above the band gap*

All of the preceding ablation was performed by focusing wavelengths to which the diamond is transparent onto the sample surface. The behavior of the ablation was expected to be different when using 213nm radiation, as the diamond is opaque to wavelengths above the band gap and thus all of the energy should be deposited at the surface. In fact, use of ps duration 213nm radiation (100μJ with a 5μm step size) results in no observable cracking or darkening of the P3 diamond surface (Fig. 9) aside from a clear delineation of some polycrystalline grain boundaries, in the optical image, with grain size consistent with the manufacturer's specification.

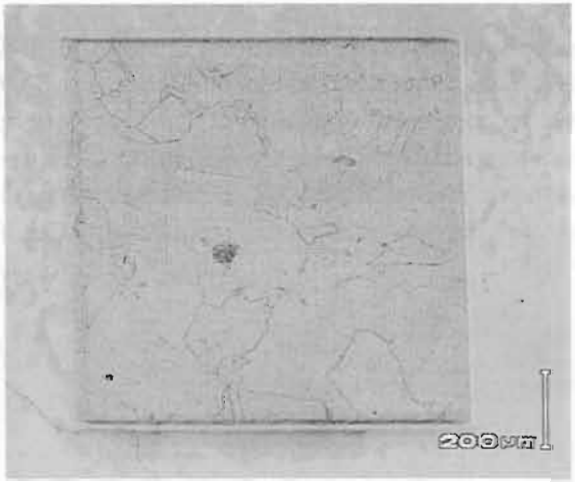


Figure 9. Optical image of P3 ablated with ~30ps 213nm radiation.

The SEM scans of this diamond can barely reveal the edges of the patterned region, even at a significant sample tilt (data not shown). AFM scans of the surface (Fig. 10) indicate that the faceting of different grains in the sample creates discontinuities across these boundaries but that within a grain, the surface variation is uniformly about 0.1μm with 5μm spacing between the ablation lines.

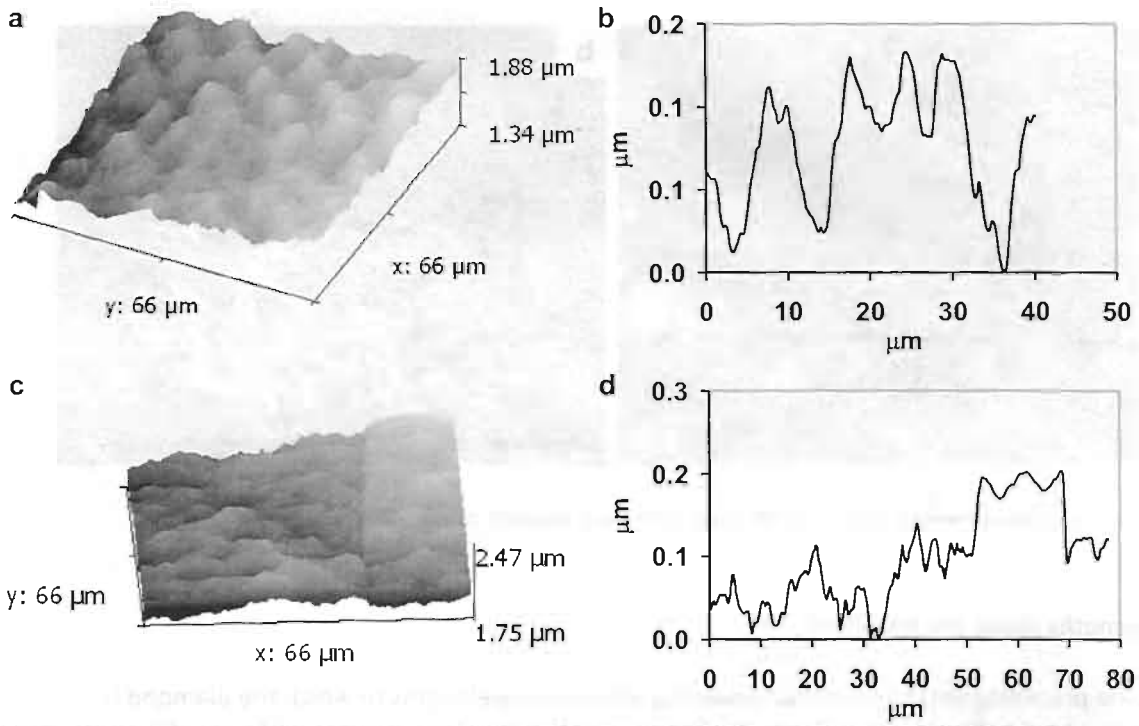


Figure 10. AFM images (left) and line scans (right) of P3 ablated with ~30ps 213nm radiation (a) in the center of a single grain and (b) across a grain boundary.

**B. Single Crystal Diamond**

*Wavelengths below the band gap*

Based on the results of the polycrystalline diamond ablation, it appeared likely that absorbance of radiation along grain boundaries was a significant source of discontinuity in the patterning, thus single-crystal diamond was patterned for comparison. Ablation of S1 was performed using 100μJ of 266nm ps-duration radiation with a 10μm step size. Four passes over a 1x4mm area were completed over 640 minutes with a 5μm offset in position for each pass. This produced a generally uniform surface, with small (~10μm wide), relatively rare crevices interspersed across the surface (Fig. 11). No cracking or surface darkening was observed.

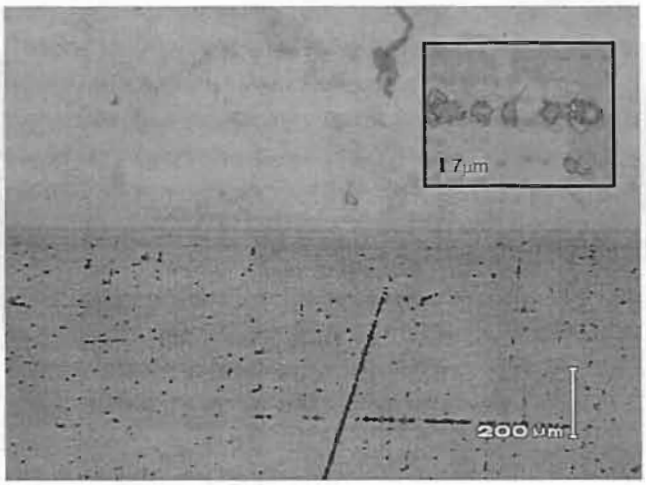


Figure 11. Optical image of S1 ablated with ~30ps 266nm radiation. Inset is expanded view of crevices in diamond.

*Wavelengths above the band gap*

A 1x1mm$^2$ square was patterned onto S2 using 100μJ of 213nm ps-duration radiation with a 5μm step size. This produced a surface smooth enough that the raster step could not be observed with SEM, but which had small darkened areas in the optical image (Fig. 12). Using higher magnification, these dark areas were revealed to be crevices <5μm in width. It is apparent from our analysis that some surface contamination was present on S2 during the ablation process, which may have caused an increase in the frequency of these crevices. Ultrasonic cleaning in acetone for 30 minutes is clearly not sufficient to obtain a clean enough diamond substrate for micron-scale patterning.

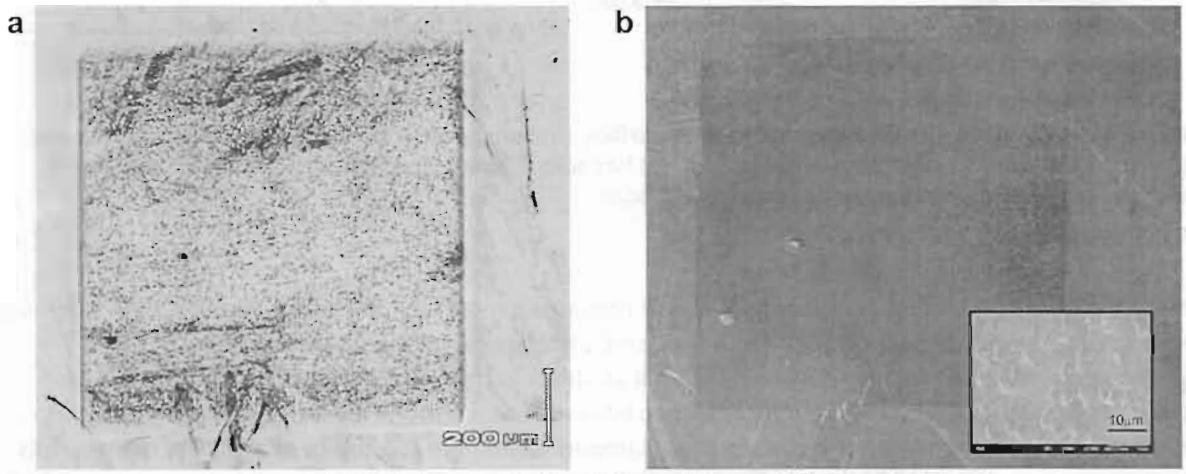


Figure 12. (a) Optical and (b) 70X SEM image of ~30ps 213nm ablation of S2. Inset in SEM image is an expanded view (2700X) of the surface.

AFM analysis (Fig. 13) of this diamond reveals a depth profile for the ablation surface with 0.1μm variation in depth along the periodic 5μm spacing of the pattern (Fig. 13c), while the crevices are almost 0.5μm deep (Fig. 13d). Analysis of the edge of the patterned area indicates that the full ablation depth (ignoring the crevices) is ~1.5μm (Fig. 13e,f).

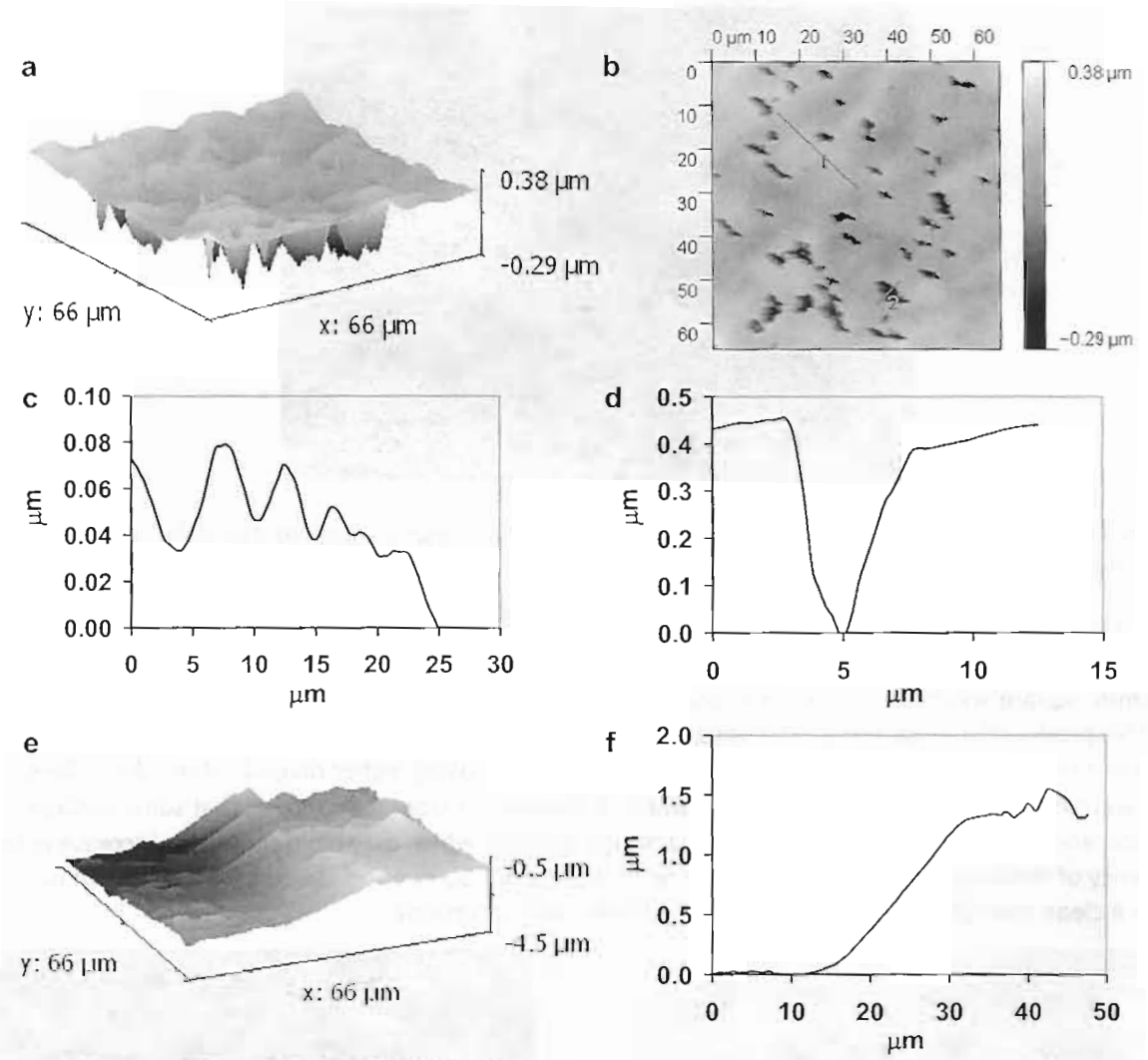


Figure 13. AFM of S2. (a) Topographical view of surface, (b) scan of surface indicating positions of line scans (1&2), (c) line scan 1 across the ablation pattern, (d) line scan 2 across the crevice, (e) topographical view of the edge of the ablation pattern, (f) line scan of the edge.

## IV. CONCLUSIONS

Ablation with above band gap radiation (213nm) provides a relatively uniform surface on both poly- and single-crystal diamond. For polycrystalline diamond, all other examined wavelengths resulted in significant cracking and surface darkening as well as stress in the diamond lattice. The non-diamond carbon which causes surface darkening is able to be removed via ozone cleaning. Detailed analyses of the strain in the diamond and the surface non-diamond carbon are the topics of separate manuscripts. For single-crystal diamond, 266nm radiation did not result in cracking, suggesting that the cracking is directly related to the presence of grain boundaries. Because the grain boundaries run through the bulk of the polycrystalline diamonds, the penetrating wavelengths (below the band gap) will be absorbed and greater thermal energy may be deposited in these regions. It is possible that the ablation itself is related to the non-thermal component of the process. Evidence for this is provided by the significant difference between effects of ps and ns duration pulses of similar laser beam parameters. If the process was entirely thermal, the total energy deposited would be the same and should have the same effect. Throughout these experiments, the ablation depth was kept to a minimum in order to retain the ability

to repolish and reuse the diamonds. It should be noted that this was done for practical purposes and that there is no obvious limitation to prevent much deeper patterning.

Future work suggested by this research includes ablation of deeper patterns with larger aspect ratios as well as more complicated patterns. In addition, ablation will be attempted using an excimer laser operating at 193nm. Since the excimer lasers typically have more UV energy per pulse with an inherent flat top energy profile and run at a higher repetition rate, we anticipate that this ablation should lead to faster ablation rates and a more uniform surface.

## ACKNOWLEDGEMENTS

The authors would like to thank John Walsh for his expert technical assistance, John Warren (Center for Functional Nanomaterials) for assistance with SEM operation and Veljko Radeka for his support. This manuscript has been authored by Brookhaven Science Associates, LLC under Contract No. DE-AC02-98CH10886 with the U.S. Department of Energy. The United States Government retains, and the publisher, by accepting the article for publication, acknowledges, a world-wide license to publish or reproduce the published form of this manuscript, or allow others to do so, for the United States Government purposes.

## REFERENCES

[1]K. Evans-Lutterodt, A. Stein, J. M. Ablett and N. Bozovic, Phys. Rev. Lett. **99**, 134801 (2007).

[2]J. Smedley, I. Ben-Zvi, J. Bohon, X. Chang, R. Grover, A. Isakovic, T. Rao and Q. Wu, *Diamond Amplified Photocathodes, in Diamond Electronics—Fundamentals to Applications II*, Mater. Res. Soc. Symp. Proc. 1039, Warrendale, PA, (2007), 1039-P09-02.

[3]J. Zhang, X. M. Meng, C. Y. Chan, Y. Wu, I. Bello, and S. T. Lee, Appl. Phys. Lett. **82**, 2622 (2003).

[4]H. W. Choi, E. Gu, C. Liu, C. Griffin, J. M. Girkin, I. M. Watson, and M. D. Dawson, J. Vac. Sci. Technol. B **23**, 130 (2005).

[5]M. Tarutani, Y. Takai, and R. Shimizu, Jpn. J. Appl. Phys., Part 2 **31**, L1305 (1992).

[6]S. Gloor, V. Romano, W. Luthy, H. P. Weber, V. V. Kononenko, S. M. Pimenov, V. I. Konov and A. V. Khomich, Appl. Phys. A: Mater. Sci. Process. **70**, 547 (2000).

[7]S. Gloor, W. Lüthy, H. P. Weber, S. M. Pimenov, E. D. Obraztsova, Diamond Rel. Mater. **7**, 607 (1998).

[8]T. George, M. C. Foote, R. P. Vasquez, E. P. Fortier and J. B. Posthill, Appl. Phys. Lett. **62**, 2880 (1993).

[9]S. K. Sudheer, V. P. Mahadevan Pillai and V. U. Nayar, J. Raman Spectrosc. **38**, 427 (2007).

[10]S. Preuss and M. Stuke, Appl. Phys. Lett. **67**, 338 (1995).

[11]J. Smedley, T. Rao, C. Jaye, D. Fischer and J. Bohon, J. Appl. Phys. **?**, ? (2009).